Properties of the giant dipole resonance built on the isobaric analog state

S. Mordechai
Ben-Gurion University of the Negev, Beer-Sheva 84105, Israel
and University of Texas at Austin, Austin, Texas 78712

N. Auerbach,* S. Greene, and C. L. Morris
Los Alamos National Laboratory, Los Alamos, New Mexico 87545

J. M. O'Donnell, H. T. Fortune, G. Liu, M. Burlein, and A. Wuosmaa
University of Pennsylvania, Philadelphia, Pennsylvania 19104

S. H. Yoo and C. Fred Moore
University of Texas at Austin, Austin, Texas 78712
(Received 17 April 1989)

Resonances were observed in pion-induced double charge exchange (at $T_\pi = 292$ MeV) on ^{13}C, ^{59}Co, ^{93}Nb, ^{138}Ba, and ^{197}Au in the continuum at excitation energies of 8.4, 27.5, 33.2, 38.7, and 44.2 MeV, respectively ($Q = -27.4$, -32.3, -35.8, -38.4, and -46.0 MeV). An angular distribution was measured for the resonance on ^{93}Nb and observed to have a dipole shape. The measured cross sections and the angular distribution agree well with a simple sequential two-step calculation in which the intermediate states arise from single charge exchange to the isobaric analog state and to the giant dipole resonance. Based on their excitation energies, angular distribution for ^{93}Nb, and cross sections we identify the resonances as the giant dipoles built on the isobaric analog states. The new data together with the recent observation of the resonance in three other nuclei indicate that the excitation energies, widths, and cross sections for these resonances have a simple mass dependence.

I. INTRODUCTION

In a recent paper[1] we reported the observation of giant dipole resonances (GDR) built on the isobaric analog states (IAS) in (π^+, π^-) double charge exchange (DCX) on ^{56}Fe, ^{nat}Se, and ^{208}Pb. The identification of these resonances is based on the characteristic dipole angular distribution for ^{56}Fe, the $A^{-1/3}$ dependence of the excitation energies, and on the ratios of cross sections to those of the double isobaric analog states (DIAS). The giant dipole resonances built on isobaric analog states (GDR⊗IAS) can be written in terms of charge-exchange dipole (D_-) and isospin-lowering operators (τ_-) acting sequentially on the ground-state wave function[1]. Therefore, for spin-zero non-self-conjugate nuclei these resonances have a single spin and parity of 1^-, and three isospin members with $T-1$, T, and $T+1$, where T is the isospin of the target nucleus. The difficulty in observing double giant resonances arises mainly from the fact that these states are located high in the continuum so that they are in a region of very high density of states and have a large width. Special kinematical and reaction conditions are thus needed to allow their observation above background. The selectivity of the double-charge-exchange reaction is such that $\Delta T = 0$ isoscalar transitions in the target nucleus that are very strongly excited in inelastic scattering have no counterparts in the nucleus $(N-2, Z+2)$; therefore the background underneath the peak is getting reduced. An example of this unique feature of pion DCX as an excellent tool to study double isovector resonances is the well-known DIAS which can be viewed in this context as the simplest double-resonance state. Until recently,[1,2] none of the higher double resonances had been observed.

Cross sections for the two ingredient resonances, the IAS (Refs. 3–5) and the GDR,[6,7] which are strongly excited in pion single charge exchange (SCX), both have a rather simple mass dependence, as discussed later. At 292 MeV, pion DCX is thought to proceed predominantly by a two step $(\pi^+, \pi^0) \otimes (\pi^0, \pi^-)$ mechanism—therefore the GDR⊗IAS should also have a simple form for the A dependence which incorporates both the GDR and the IAS systematics.

In the present work we report on new observations of the GDR⊗IAS in five additional nuclei covering a wide range of mass. The results from the present study and previous work[1] indicate that these resonances are a general feature of all nuclei with $N - Z \geq 1$. We will also discuss the systematics of the energies, widths, and cross sections of these newly observed resonances as a function of A. These give insight on their structure in terms of a charge-exchange GDR built on the isobaric analog state or vice versa.

II. EXPERIMENT

The measurements were performed with the energetic pion channel and spectrometer (EPICS) at Clinton P. Anderson Meson Physics Facility (LAMPF) with the standard pion double-charge-exchange setup.[8] The isotopic purity and areal density of the targets used in the present and previous experiments are listed in Table I. Measurements were taken at $T_\pi = 292$ MeV and a scattering angle of 5°. An angular distribution was measured on ^{93}Nb at scattering angles 5°–30° in 5° steps. Electrons were eliminated using a freon-gas velocity-threshold Cherenkov detector in the focal plane. A scintillator placed behind a series of graphite blocks was used to detect and veto muon events.[9] The remaining background was pions resulting from continuum DCX on the target. The choice of the highest beam energy available at EPICS ($T_\pi = 292$ MeV) for the present measurements had three advantages: (a) a lower background level from the continuum DCX spectra since the excitation-energy region of interest is away from the inclusive DCX peak, (b) a large outgoing energy range ($\approx$ 50 MeV) is covered by the acceptance of the spectrometer in a single setting, and (c) cross sections are expected to increase as k^2 or faster.

The acceptance of the spectrometer was measured by pion scattering from ^{12}C at a given angle by varying the spectrometer field to cover an outgoing pion momentum range of about ±10% of the central momentum of the spectrometer. Absolute normalizations were obtained by measuring π–p scattering from a polyethylene (CH_2) target of areal density 25.7 mg/cm^2 and comparing the yields with cross sections calculated by π-nucleon phase shifts in Ref. 10.

III. RESULTS AND ANALYSIS

A. Discussion of the data

Figure 1 shows the ^{93}Nb Q-value spectra at two angles. In addition to the DIAS at $E_x = 19.3$ MeV ($Q = -21.9$ MeV), both spectra show the existence of a relatively wider peak located in the continuum region at about 13.9 MeV above the DIAS. This peak is labeled GR in the figure. The DIAS is strong at 5° but very weak at 10°, whereas the GR has almost equal strength at the two angles. The peaks were fitted with a Gaussian and a Lorentzian shape of variable widths for the DIAS and the GR, respectively. In Fig. 1 we show a fit to the spectra with $\Gamma_{DIAS} = 1.6$ MeV and $\Gamma_{GR} = 5.8$ MeV. The spectra can be well fitted also using a Gaussian line shape for the GR, resulting in a smaller cross section by about 50%. The width of the DIAS arises primarily from resolution energy due to the thick (1.714 g/cm^2) ^{93}Nb target. The spectra have been corrected for the spectrometer acceptance as a function of momentum. The background (dashed line), which arises from DCX to discrete low-lying states and to the continuum, was fitted using a third-order polynomial shape of the form

$$R(1) + R(2)E + R(3)E^2 + R(4)E^3$$

where E is the Q value. It was found that comparable fits and cross sections are obtained if, instead, fourth-

TABLE I. Target compositions and areal densities.

Target	Isotopic purity (%)	Areal density (g/cm^2)
^{13}C	90	0.329
^{56}Fe[a]	91.8	1.199
^{59}Co	100	1.079
^{80}Se[a]	49.8	1.86
^{93}Nb	100	1.714
^{138}Ba	>99	0.327
^{197}Au	100	1.000
^{208}Pb[a]	>99	0.516

[a]Reference 1.

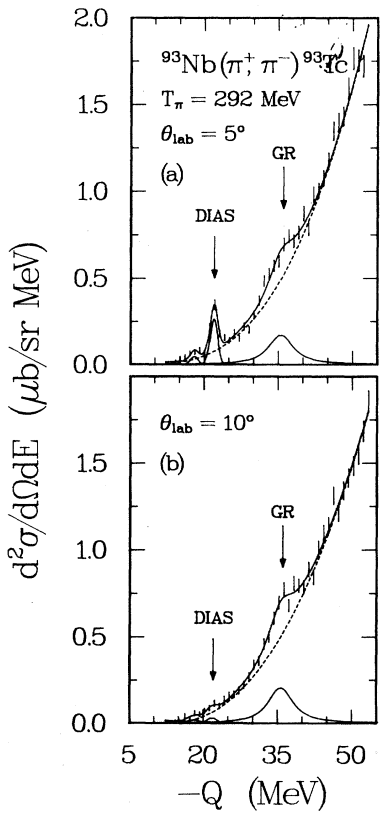

FIG. 1. Double differential cross-section spectrum for (π^+, π^-) reaction on a ^{93}Nb target at $T_\pi = 292$ MeV: (a) $\theta_{lab} = 5°$, and (b) $\theta_{lab} = 10°$. The arrows indicate the fitted location of the DIAS and the giant resonance (GR). Short vertical lines represent statistical uncertainty of the data. The dashed line is the fitted background with a polynomial shape and the solid line is the fit to the spectrum with the use of NEWFIT.

or higher-order polynomial shapes are used for the background. The solid line is the resulting fit to the spectrum.

Figure 2 presents the angular distribution extracted for the GR on ^{93}Nb at 292 MeV. The maximum cross section is observed at 10° with a smaller cross section at 5° and 15°. At scattering angles of 20°–25° the resonance is very weak and can hardly be observed, but at 30° the peak shows up again above background. The solid and dashed lines in Fig. 2 are simple calculations in which sequential single charge exchange through the isobaric analog to the giant dipole resonance is evaluated with two different transition densities for the IAS (Refs. 1 and 11) and will be discussed later.

Figure 3(a) shows the ^{138}Ba Q-value histogram. Again in addition to the narrow transition to the DIAS at $E_x = 27.7$ MeV ($Q = -27.4$ MeV), the spectrum shows the existence of a clear and wider peak labeled GR at about 11.0 MeV above the DIAS sitting on a large background from the continuum. The figure shows a fit to the spectrum with $\Gamma_{\rm DIAS} = 0.25$ MeV (Ref. 12) (after subtracting the resolution energy) and $\Gamma_{\rm GR} = 6.8$ MeV using a Gaussian line shape for the first and a Lorentzian for the second. The background (dashed line) is a third-order polynomial shape. The confidence level for the observed resonances is about seven (greater than nine) standard deviations in the individual spectra on ^{93}Nb (^{138}Ba) shown in Fig. 1 [Fig. 3(a)], respectively. The 5° spectra for ^{59}Co and ^{197}Au look quite similar to those shown on ^{93}Nb and ^{138}Ba. An exception is the ^{13}C($T = \frac{1}{2}$) target. Figure 3(b) shows the 5° DCX spectrum on the enriched ^{13}C target. The spectrum has a strong nonanalog transition to the ground state of ^{13}O ($Q = -19.0$ MeV), and a wider peak at about 8.4 MeV above the ground state ($Q = -27.4$ MeV). In this case the DIAS does not exist and the GDR⊗IAS is reduced in strength. We will return to this point in Sec. III C.

B. Energies and widths of the GDR built on the IAS

Table II summarizes the deduced energies, widths, and cross sections for the GR observed in the present study and those reported recently on ^{56}Fe, $^{\rm nat}$Se, and ^{208}Pb[1]. For $T \geq 1$ target nuclei, the $\Delta T_z = -1$ charge-exchange isovector giant dipole and the GDR⊗IAS split into three members (Fig. 4) with isospin $T-1$, T, and $T+1$. The energy splitting between members $\Delta E^-(T, T-1)$ and $\Delta E^+(T+1, T)$ is a function of T and A and was discussed in Refs. 13 and 14. Table II lists the energies, widths, and cross sections of the GR peaks when fitted as a whole with a single Lorentzian peak with the given width. The data from Ref. 1 have been refitted under

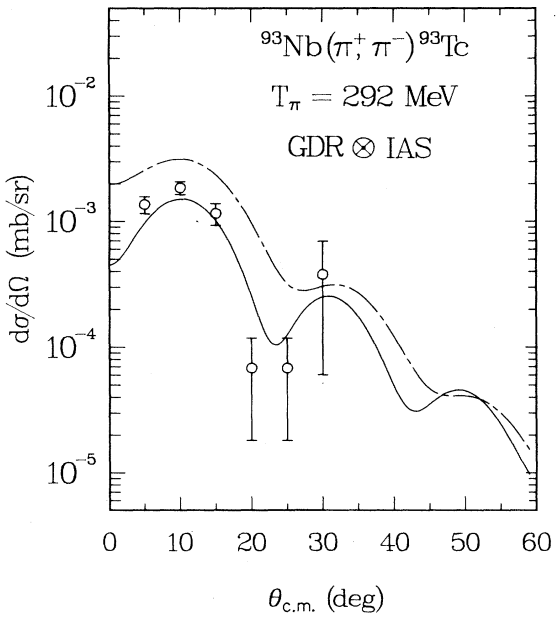

FIG. 2. Angular distribution for the peak labeled GR in the double-charge-exchange spectrum on ^{93}Nb shown in Fig. 1. The cross sections have been extracted with use of a Lorentzian line shape for the giant resonance with constant width of 5.8 MeV and constant $Q = -35.8$ MeV ($E_x = 33.2$ MeV). The solid and chain dashed lines are sequential model calculations with use of surface and volume transition densities, respectively, without any normalization factor.

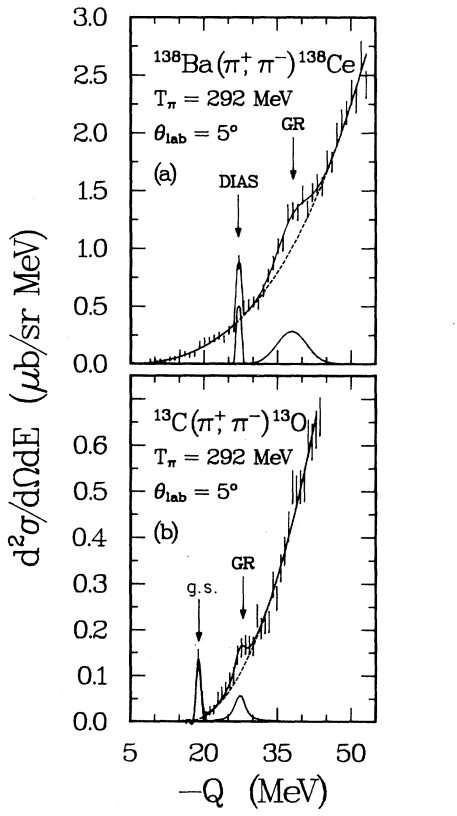

FIG. 3. (a) Same as Fig. 1(a) except for enriched ^{138}Ba target. (b) Same as above except for enriched ^{13}C target and a bin size of 0.8 MeV. The arrows indicate the fitted location of the ground state (g.s.) and the giant resonance (GR).

TABLE II. Results from the double-charge-exchange reaction from the present and previous work at an incident pion energy $T_\pi = 292$ MeV. Cross sections are at the listed laboratory angles.

			Experiment[a]		
Target	Q(DIAS) (MeV)	Q(GR) (MeV)	Γ(GR) (MeV)	θ_{lab} (deg)	$\frac{d\sigma}{d\Omega}$(GR) (μb/sr)
^{13}C		−27.4±0.5	2.0±1.0[b]	5	0.14±0.06
^{56}Fe	−15.6 ±0.1	−34.7±0.6	7.1±2.0	12	1.15±0.19
^{59}Co	−15.9 ±0.1	−32.3±1.1	7.2±3.4	5	0.90±0.33
^{80}Se	−18.8 ±0.1	−33.7±0.6	5.3±2.5	5	3.40±0.80
^{93}Nb	−21.9 ±0.1	−35.8±0.5	5.8±1.0	10	1.88±0.27
^{138}Ba	−27.38±0.07	−38.4±0.4	6.8±1.6	5	3.44±0.37
^{197}Au	−34.9 ±0.1	−46.0±0.8	9.0±1.6	5	5.43±1.7
^{208}Pb	−35.6 ±0.1	−45.8±0.8	8.6±1.9	5	8.61±1.1

[a]Cross sections, energies, and widths for the GDR built on the IAS obtained by fitting the GR with a single Lorentzian peak with the listed widths. Data from Ref. 1 have been refitted under the same conditions.

[b]After correcting for the resolution.

the same conditions. For ^{13}C the listed cross section is for the $(T+1)$ member, since the lower two components are forbidden from isospin considerations.

Table III lists the predicted intensity ratios for the GDR⊗IAS members in DCX, derived from simple isospin arguments.[11] These ratios are quite different from the ratios expected for a GDR in SCX where the dipole is in a $T_z = T-1$ nucleus.[15] We note, however, that for both SCX and DCX reactions on neutron-rich nuclei the transition to the lowest isospin member of the multiplet is dominant and the higher two components are generally negligible. The T and $T+1$ components are further suppressed by Pauli blocking which is not included in the calculated intensity ratios. Table IV lists the predicted cross sections for the GDR⊗IAS made using simple sequential-model calculations, using the pion coupled-channels impulse-approximation (CCIA) code NEWCHOP.[16] The calculations include the ground state, the GDR, the IAS, and the GDR⊗IAS. The strength of each SCX transition has been adjusted to reproduce the measured (or extrapolated) SCX cross section to the GDR and the IAS. A collective transition density was used for the dipole. For the IAS we used two different transition densities—one volume (model I) and one surface peaked (model II). The calculations using model II for the IAS, which provide a more realistic shape for the excess density, ρ_{exc}, give quantitatively a good description of the measured cross sections. The calculations

TABLE III. Intensity ratios for isovector excitations in pion double charge exchange, assuming equal reduced matrix elements.

			Isospin members[a]		
Target	$\|T,T_z\rangle_i$	$\|T,T_z\rangle_f$	$\|T_i-1\rangle$	$\|T_i\rangle$	$\|T_i+1\rangle$
^{13}C	$(\frac{1}{2},\frac{1}{2})$	$(\frac{3}{2},-\frac{3}{2})$			1.0
^{56}Fe[b]	(2,2)	(0,0)	0.3	0.5	0.2
^{59}Co	$(\frac{5}{2},\frac{5}{2})$	$(\frac{1}{2},\frac{1}{2})$	0.4	0.46	0.14
^{80}Se	(6,6)	(4,4)	0.72	0.26	0.03
^{93}Nb	$(\frac{11}{2},\frac{11}{2})$	$(\frac{7}{2},\frac{7}{2})$	0.68	0.28	0.04
^{138}Ba	(13,13)	(11,11)	0.85	0.14	0.01
^{197}Au	$(\frac{39}{2},\frac{39}{2})$	$(\frac{35}{2},\frac{35}{2})$	0.81	0.18	0.01
^{208}Pb	(22,22)	(20,20)	0.91	0.08	0.003

[a]Cross section ratios have been calculated (Ref. 11) using the relations,

$$\sigma(T-1):\sigma(T):\sigma(T+1)=\frac{(2T-1)(T-1)}{T(2T+1)}:\frac{(2T-1)}{T(T+1)}:\frac{3}{(2T+1)(T+1)}.$$

The T and $T+1$ members are further suppressed by Pauli blocking, not included in the listed ratios.

[b]Using different reduced matrix elements taken from SCX on ^{60}Ni (Ref. 6) (same isospin as ^{56}Fe) gives intensity ratios:

$$|T_i-1\rangle : |T_i\rangle : |T_i+1\rangle = 0.41 : 0.48 : 0.11.$$

TABLE IV. Theoretical and experimental peak cross sections.

Target	$\theta_{c.m.}$(peak) (deg)	Theory[a] Model I $d\sigma/d\Omega$(GR) (μb/sr)	Model II $d\sigma/d\Omega$(GR) (μb/sr)	Experiment[b] $d\sigma/d\Omega_{peak}$(GR) (μb/sr)	$\frac{d\sigma/d\Omega_{peak}(GR)}{(N-Z)NZ}$ (nb/sr)
^{13}C	16	0.21	0.13	0.17±0.07	4.05 ±1.67
^{56}Fe	11	1.70[c]	1.28	1.29±0.21	0.41 ±0.07
^{59}Co	11	1.71[c]	1.07	1.28±0.46	0.29 ±0.10
^{80}Se	10	3.13	2.24	4.15±0.98	0.22 ±0.05
^{93}Nb	10	2.56	1.84	1.88±0.27	0.10 ±0.015
^{138}Ba	9	5.95	3.32	4.20±0.45	0.035±0.004
^{197}Au	9	11.35	5.65	6.59±2.06	0.018±0.006
^{208}Pb	9	12.93	6.29	10.50±1.34	0.023±0.003

[a]Sequential model calculations using volume transition density (model I) and surface transition density (model II) for the isobaric analog state, normalized to the pion single-charge-exchange data.

[b]Peak cross sections obtained by normalizing the 5° data points from Table II to the calculated sequential model curve using NEWCHOP, and corrected for ^{56}Fe and ^{59}Co for isospin components.

[c]Corrected for the $|T_i+1\rangle$ isospin component [12% for ^{56}Fe (footnote b of Table III), 16% for ^{59}Co]. We assume that the cross sections listed in Table II (column 6) include predominantly the $|T_i-1\rangle$ and $|T_i\rangle$ components. For the heavy nuclei ($A \geq 80$) the $|T_i+1\rangle$ component is negligible.

with model I, generally, overpredict the measured cross sections for the GDR⊗IAS. More details on these calculations are given in Refs. 1 and 11. The experimental cross sections listed in Table IV are the estimated peak cross sections obtained by normalizing the 5° data points to the theoretical curves. They also have been normalized upward to account for the unobserved $T_>$ isospin component for ^{56}Fe and ^{59}Co using the ratios listed in Table III.

The energy of the $T = T_0-1$ member of the $\Delta T_z = -1$ GDR (where T_0 is the isospin of the target nucleus) is related by symmetry energy to the "normal" ($T = T_0$) GDR in the target nucleus observed, for example, in photonuclear reactions. Figure 4 illustrates (for target nuclei with $T > 1$) the relation between the dipole energy in inelastic or photonuclear reactions and the charge-exchange modes. For $T = 1$ target nuclei the lowest member of the GDR⊗IAS is forbidden, and for $T = \frac{1}{2}$ only the highest ($T = \frac{3}{2}$) member is allowed. Table V gives a comparison between E_{GDR} derived from DCX (column 6) and the corresponding energies measured or extrapolated from photonuclear reactions (column 9). The table indicates that the excitation energies of the GR above the DIAS plus the symmetry energy (ΔE^-) are in close agreement with the electric giant dipole energies, and can be well represented with either an $A^{-1/3}$ or $A^{-1/6}$ dependence (times a constant 76.6±1.5 and 35.0±0.6 MeV, respectively). These systematics are shown in Fig. 5 and give strong support to the identification of the GR peaks observed in DCX in the present work as giant dipole oscillations built on the isobaric analog as intermediate states. It is known from photonuclear reactions that $A^{1/3}$ is too strong and $A^{1/6}$ is too weak an A dependence for $E1$ energies. Figure 5 shows that the GDR energies derived from DCX are also consistent with this feature. In the case of ^{13}C we deduce the $E1$ energy by subtracting $2(\Delta E_C - \delta)$ from the measured Q value for the GR, where we have used $\Delta E_C = 1.44 \times (Z_< + \frac{1}{2})/A^{1/3} - 1.13$ MeV for the Coulomb displacement energy[17] and $\delta = m_n - m_p$. This procedure yields $E1(T_>) = 27.4 - 3.8 = 23.6$ MeV for ^{13}C. This is in good agreement with the centroid energy of 23.8 MeV for the $T_> = \frac{3}{2}$ component of the GDR on ^{13}C reported in the ^{13}C(γ,p) reaction.[18] Figure 6 shows a plot of the ratio $\Gamma_{T<}/A$, where $\Gamma_{T<}$ is the width of the lowest isospin member of the GDR⊗IAS for ^{56}Fe, ^{59}Co, and ^{80}Se (in which the $T_<$ component is resolved) and the whole GR width for ^{93}Nb, ^{138}Ba, ^{197}Au, and ^{208}Pb

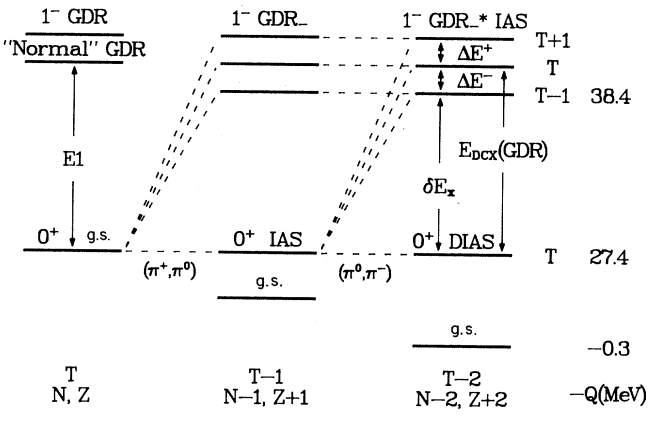

FIG. 4. Schematic energy-level diagram of analog and dipole states observed in single and double charge exchange, compared with the $E1$ resonance in the target from photonuclear reactions. The listed Q values refer to the case of DCX on ^{138}Ba.

TABLE V. Giant dipole energies derived from DCX compared with results from photonuclear reactions.

Target	$Q_{T_<}$(GR)[a] (MeV)	$\Gamma_{T_<}$(GR)[b] (MeV)	δE_x[c] (MeV)	ΔE^-[d] (MeV)	E_{DCX}^{GDR}[e] (MeV)	$E_{DCX}^{GDR} A^{1/3}$ (MeV)	$E_{DCX}^{GDR} A^{1/6}$ (MeV)	E_{photo}^{GDR}[f] (MeV)
^{13}C					23.6±1	55.5±2.4	36.2±1.5	23.8[g]
^{56}Fe	−31.8±0.6	3.5±1.4	16.2±0.7	1.8	18.0±0.6	68.8±2.3	35.2±1.2	17.6[h]
^{59}Co	−29.8±0.5	3.5±1.0	13.9±0.6	2.1	16.0±0.6	62.3±2.3	31.6±1.2	17.2[h]
^{80}Se	−33.3±0.5	4.1±2.2	14.5±0.7	3.5	18.0±0.7	77.6±3.0	37.4±1.5	17.1[i]
^{93}Nb	−35.8±0.5	5.8±1.0	13.9±0.6	2.7	16.6±0.6	75.2±2.7	35.3±1.3	16.6
^{138}Ba	−38.4±0.4	6.8±1.6	11.0±0.5	3.6	14.6±0.6	75.4±3.1	33.2±1.4	15.3
^{197}Au	−46.0±0.8	9.0±1.6	11.1±0.9	2.5	13.6±0.9	79.1±5.2	32.8±2.2	13.8
^{208}Pb	−45.8±0.8	8.6±1.6	10.3±0.9	2.2	12.5±0.9	74.1±5.3	30.4±2.2	13.5

[a]Energy of the $T_< = T_0 - 1$ component of the GDR⊗IAS for ^{56}Fe, ^{59}Co, and ^{80}Se where it is resolved. Energy of the whole resonance for the heavier nuclei (^{93}Nb, ^{138}Ba, ^{197}Au, and ^{208}Pb).

[b]Same as footnote a except for widths.

[c]$\delta E_x = Q(\text{DIAS}) - Q_{T_<}(\text{GR})$ (see Ref. 22).

[d]$\Delta E^- = T[E_v - (2T+3)E_t]$; $E_v = 50/A$, and $E_t = -0.003$ (Ref. 14). We note that for ^{56}Fe this relation gives a smaller value for ΔE^- than observed in Ref. 11.

[e]$E_{DCX}^{GDR} = \delta E_x + \Delta E^-$.

[f] $E1$ energies generally include combination of $E_<$ and $E_>$ (Ref. 21).

[g]Centroid energy of the $T_>$ component of the GDR (Ref. 18).

[h]$E1$ on ^{65}Cu (Ref. 21), scaled by $A^{1/3}$.

[i]$E1$ on ^{nat}Rb (Ref. 21), scaled by $A^{1/3}$.

where the resonance is dominated by the lowest isospin component. These widths are listed in column 3 of Table V as a function of A. The figure indicates that for $A \geq 56$ the width of the lowest component of the GDR⊗IAS is approximately linear with A, and can be represented by $\Gamma_{T_<}(\text{GR}) = (0.048 \pm 0.004)A$ MeV.

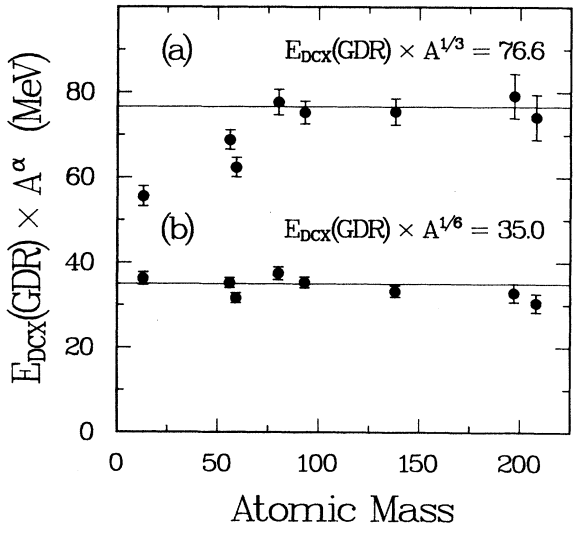

FIG. 5. (a) Giant-dipole resonance energies derived from DCX (corrected for the symmetry energy) multiplied by $A^{1/3}$ plotted versus mass number. The line is the best constant fit to the data for $A \geq 80$. (b) Same as in (a) except that the GDR energies derived from DCX are multiplied by $A^{1/6}$. The line is a fit to all eight data points.

C. Mass dependence of the GDR built on the IAS

We now address the A dependence of the cross section of the GDR⊗IAS in view of the existing knowledge on the GDR and the IAS from pion SCX reactions. The isobaric analog state has been studied extensively using the (π^+, π^0) charge exchange reaction.[3–5] Figure 7 shows some of the regularities of the 0° IAS cross sections at 165 and 300 MeV. The data could be well represented[5] by

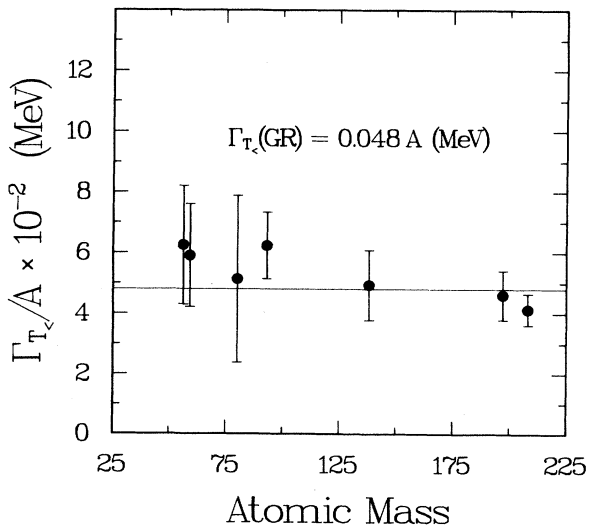

FIG. 6. Widths of the lowest member of the giant dipole resonance built on the isobaric analog state ($\Gamma_{T_<}$) divided by A plotted versus mass number (see text).

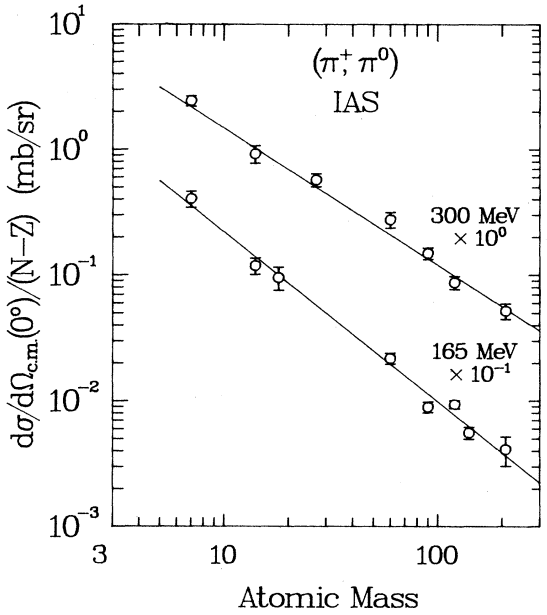

FIG. 7. The A dependence of 0° SCX cross sections for the isobaric analog state at 165 and 300 MeV. The lines represent fits of the function $g_1(N-Z)A^{-\alpha}$ to the data. The data are taken from Refs. 4 and 5.

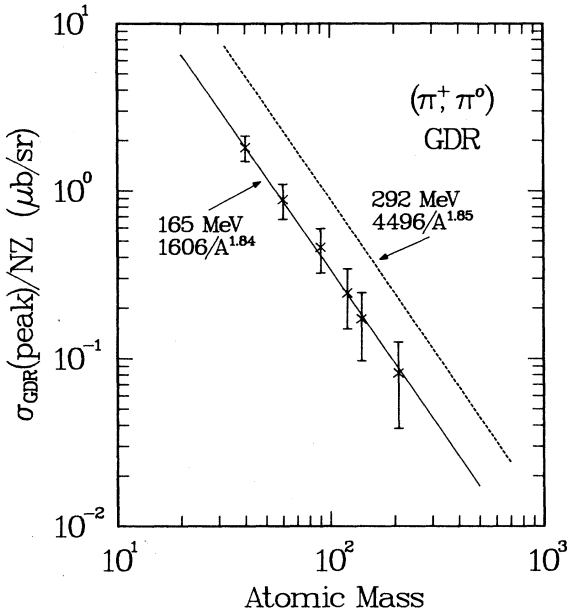

FIG. 8. Normalized GDR peak cross sections obtained in the (π^+, π^0) reaction at 165 MeV as a function of A. The data are taken from Ref. 6. The solid line is a fit at 165 MeV, Eq. (3), and the dashed line is a theoretical calculation for the GDR at 292 MeV, Eq. (5) (see text).

$$\left(\frac{d\sigma}{d\Omega}\right)_{\rm IAS}(0°) = g_1(N-Z)A^{-\alpha}\,, \tag{1}$$

where the $(N-Z)$ arises from the fact that the reaction occurs only on valence neutrons. The $A^{-\alpha}$ is due to pion attenuation and is energy dependent. At 165 MeV, α is 1.36 but it decreases as one moves away from the $\Delta_{3/2,3/2}$ resonance region where pion absorption effects are weaker. At 300 MeV, the best representation to the data is given by[5]

$$\left(\frac{d\sigma}{d\Omega}\right)_{\rm IAS}(0°) = (18.0 \pm 1.7)(N-Z)A^{-1.09} \quad \text{mb/sr}\,. \tag{2}$$

The $S = 0\tau_-$ (τ_+) mode of the GDR has been observed to be strongly populated in the (π^+, π^0) [(π^-, π^0)], charge exchange reaction.[6,7] Figure 8 shows the existing (π^+, π^0) SCX data to the GDR at 165 MeV. Except for the GDR on the ^{40}Ca target, which has only one ($T = 1$) isospin member, the GDR cross sections on the heavier targets ($N \neq Z$) (shown in Fig. 8) include all three isospin members ($T-1$, T, and $T+1$) which are not resolved with the π^0 spectrometer.[6] These three members have different reduced matrix elements due to Pauli blocking which favors the lowest member. Our best fit to the summed GDR cross sections gives

$$\left(\frac{d\sigma}{d\Omega}\right)_{\rm GDR}(\text{peak}) = (1606 \pm 27)\frac{NZ}{A^{1.84}} \quad \mu\text{b/sr}\,, \tag{3}$$

where we have included the expected NZ factor. This relation is in close agreement with calculations for the $T = T_0$, $\Delta S = 0$ GDR in the strong absorption approximation which gives[19]

$$\left(\frac{d\sigma}{d\Omega}\right)_{\rm GDR}(\Delta S = 0) \simeq \frac{NZ}{A^2}\,. \tag{4}$$

Both Eq. (3) derived from the data and Eq. (4) derived from theory imply a very weak A dependence at the maximum cross section since $NZ \simeq A^2$. Since no SCX data exist for the GDR at 292 MeV, we calculated the GDR at this energy using the code NEWCHOP (Ref. 16) with dipole transition strengths adjusted to give the experimental peak cross sections at 165 MeV. This method was tested by calculating the energy dependence of the SCX cross section for the GDR and is discussed in Ref. 11. The calculated GDR cross sections at 292 MeV (dashed line) are well represented by

$$\left(\frac{d\sigma}{d\Omega}\right)_{\rm GDR}(\text{peak}) = 4496\frac{NZ}{A^{1.85}} \quad \mu\text{b/sr}\,. \tag{5}$$

Thus, except for a scaling factor (of about 2.8), the calculations at 292 MeV predict virtually the same A dependence for the GDR as is experimentally observed at 165 MeV. The increase in the GDR cross section with energy is due to a k^2 factor, where k is the incoming pion momentum, and is discussed in Ref. 7.

If we use the $E1$ classical sum rule for the dipole:[20]

$$S(E1) = 14.8\frac{NZ}{A} = |M(E1)|^2\ E\ \ e^2\,\text{fm}^2\,\text{MeV}\,, \tag{6}$$

where $|M(E1)|^2$ is the dipole transition strength, then in similarity to the IAS, one can factor the GDR cross

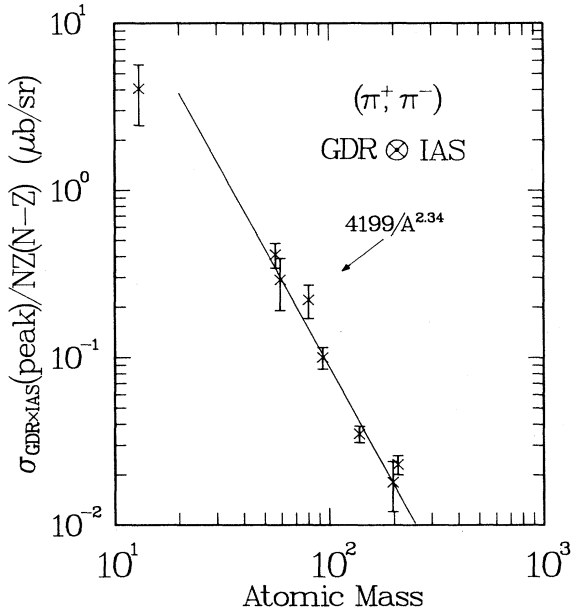

FIG. 9. Plot of normalized cross section vs A for the giant dipole built on the isobaric analog state (Table IV, column 6) measured in the present and previous DCX reactions at 292 MeV. The line is a power-law fit to the data [Eq. (8)] excluding the ^{13}C data point (see text).

section as strength times an attenuation factor:

$$(d\sigma/d\Omega)_{GDR} \approx |M(E1)|^2 A^{-\alpha} = 14.8 \frac{NZ}{AE} A^{-\alpha} . \quad (7)$$

Then, if the dipole energy varies as $A^{-1/3}$, results of Eq. 5 together with Eq. 7 give $\alpha = 1.18$. This result is in close agreement with the pion attenuation observed at this energy for the IAS, Eq. (2).

Including the present data, the existing data on the GDR⊗IAS consist of the eight data points listed in Table II. The experimental peak cross sections (Table IV) are well represented (Fig. 9) by the function,

$$\left(\frac{d\sigma}{d\Omega}\right)_{GDR\otimes IAS} (\text{peak}) = 4199(N-Z)\frac{NZ}{A^{2.34}} \quad \mu\text{b/sr} . \quad (8)$$

The ^{13}C data point is too small by about a factor of 2 or 3 in the A-dependence plot. The relatively small cross section for the GDR⊗IAS in this case is due to the fact that from isospin considerations the resonance on ^{13}C can be reached only through the IAS or the $T_>$ GDR as an intermediate state. Therefore, in this case the coupling through the GDR has only $\frac{1}{3}$ of its normal strength. On the other hand, for all heavier nuclei studied in the present experiment the GDR⊗IAS arises by coupling through both the IAS and the full GDR intermediate states. Therefore in Fig. 9, we exclude the ^{13}C data point from the fit.

The result of Eq. (8) is interesting in view of the regularities for the IAS and the GDR pointed out earlier. It is likely that the $(N-Z)$ arises from the IAS transition, Eq. (2), and the NZ factor from the GDR form factor, Eq. (3). One can similarly break the cross section for the GDR⊗IAS as the product of the strengths of the first and second step times an overall attenuation factor for DCX:

$$\left(\frac{d\sigma}{d\Omega}\right)_{GDR\otimes IAS} \approx (N-Z)\frac{NZ}{A^{2/3}} A^{-\alpha'} \quad (9)$$

A comparison of Eqs. (8) and (9) yields $\alpha' = 1.67$. This is an interesting result which indicates that for pion DCX, where three pion propagations are involved, α' is about 50% larger than for SCX (leading to the GDR or the IAS) in which only two pion propagations are involved in the reaction.

IV. SUMMARY

In conclusion, we have reported the observation of a charge-exchange giant dipole resonance built on the isobaric analog state in pion double-charge-exchange scattering on ^{13}C, ^{53}Co, ^{93}Nb, ^{138}Ba, and ^{197}Au. The $E1$ energies derived from DCX in the present and previous studies are consistent with an $A^{-1/3}$ or $A^{-1/6}$ dependence, and agree (after correcting for the symmetry energy) with the results from photonuclear reactions. The ^{93}Nb angular distribution has a clear dipole shape. Simple sequential-model calculations with collective transition densities give quantitatively a correct description of the measured cross sections. The data from the present and recent observations indicate that the newly discovered resonance is a general collective feature of all nuclei with $N-Z \geq 1$ and has a simple mass dependence which seems to incorporate the two ingredient resonances, the isobaric analog resonance, and the giant dipole resonance.

ACKNOWLEDGMENTS

We thank David Bowman for stimulating discussions. This work is supported by the U.S.–Israel Binational Science Foundation, the Robert A. Welch Foundation, the U.S. Department of Energy, and the National Science Foundation.

*Permanent address: Tel Aviv University, Tel Aviv, Israel.

[1] S. Mordechai *et al.*, Phys. Rev. Lett. **60**, 408 (1988).
[2] S. Mordechai *et al.*, Phys. Rev. Lett. **61**, 531 (1988).
[3] H. W. Baer, in Nuclear Spectroscopy and Nuclear Reactions, Proceedings of the International Symposium, Osaka, Japan, 1984 (unpublished).
[4] U. Sennhauser *et al.*, Phys. Rev. Lett. **51**, 1324 (1983).
[5] S. H. Rokni *et al.*, Phys. Lett. B **202**, 35 (1988).

[6]A. Erell *et al.*, Phys. Rev. C **34**, 1822 (1986).
[7]F. Irom *et al.*, Phys. Rev. C **34**, 2231 (1986).
[8]H. A. Thiessen *et al.*, Los Alamos Scientific Laboratory Report No. LA-6663-MS, 1977 (unpublished); S. J. Greene *et al.*, Phys. Lett. **88B**, 62 (1979).
[9]C. L. Morris *et al.*, Nucl. Instrum. Methods A **238**, 94 (1985).
[10]G. Rowe, M. Salomon, and R. H. Landau, Phys. Rev. C **18**, 584 (1978).
[11]S. Mordechai, N. Auerbach, H. T. Fortune, C. L. Morris, and C. Fred Moore, Phys. Rev. C **38**, 2719 (1988).
[12]J. M. O'Donnell, H. T. Fortune, J. D. Silk, S. Mordechai, C. L. Morris, J. D. Zumbro, S. H. Yoo, and C. Fred Moore (unpublished).
[13]R. Leonardi, Phys. Rev. C **14**, 385 (1976).
[14]N. Auerbach, A. Klein, and N. V. Giai, Phys. Lett. **106B**, 347 (1981).
[15]R. Leonardi, in *Pion-Nucleus Physics: Future Directions and New Facilities at LAMPF*, Proceedings of the Los Alamos Conference on Pion-Nucleus Physics, AIP Conf. Proc. No. 163, edited by R. J. Peterson and D. D. Strottman (AIP, New York, 1987), p. 321.
[16]E. Rost, computer code CHOPIN (unpublished). The code has been modified by one of us (C.L.M.) to calculate pion charge exchange reactions and renamed NEWCHOP.
[17]J. D. Anderson, C. Wong, and J. W. McClure, Phys. Rev. **138**, B615 (1965); M. S. Antony, J. Britz, J. B. Bueb, and A. Pape, At. Data Nucl. Data Tables **33**, 447-478 (1985).
[18]D. Zubanov *et al.*, Phys. Rev. C **27**, 1957 (1983).
[19]Avraham Gal, Phys. Rev. C **25**, 2680 (1982).
[20]A. Bohr and B. Mottleson, Nucl. Phys. **II**, 403 (1975).
[21]B. L. Berman and S. C. Fultz, Rev. Mod. Phys. **47**, 713 (1975).
[22]For ^{93}Nb, ^{138}Ba, ^{197}Au, and ^{208}Pb, δE_x listed in Table V is defined as $\delta E_x = Q(\mathrm{DIAS}) - Q(\mathrm{GR, whole\ peak})$ rather than the difference between Q(DIAS) and $Q_{T_<}$(GR). With this new definition it is easy to see that $E_{\mathrm{DCX}}(\mathrm{GDR}) = \delta E_x + S_{T_<}\Delta E^- - S_{T_>}\Delta E^+$, where $S_{T_<}$ and $S_{T_>}$ are the relative strengths of the $|T_i - 1\rangle$ and $|T_i + 1\rangle$ components, respectively, listed in Table III. The Pauli blocking effect will further increase $S_{T_<}$ and decrease $S_{T_>}$. Thus, in all the above cases the third term is negligible. Using the relation, $E_{\mathrm{DCX}}(\mathrm{GDR}) = \delta E_x + S_{T_<}\Delta E^-$, we obtain, E_{DCX}(GDR)=15.74, 14.1, 13.1, and 12.3 MeV, for ^{93}Nb, ^{138}Ba, ^{197}Au, and ^{208}Pb, respectively. In Table V we assumed $E_{\mathrm{DCX}}(\mathrm{GDR}) = \delta E_x + \Delta E^-$, i.e., $S_{T_<} = 1.0$.